

Macromolecules

Volume 26, Number 17

August 16, 1993

© Copyright 1993 by the American Chemical Society

Aromatic Copolyesters with Stilbene Mesogenic Groups. 1. Liquid Crystalline Properties of Compounds Containing a Stilbene, Terephthaloyl, or Hydroquinone Central Group

Jean Pierre Leblanc,[†] Martine Tessier,[†] Didier Judas,[†] Claude Friedrich,[‡]
Claudine Noël,^{*,§} and Ernest Maréchal[†]

Laboratoire de Synthèse Macromoléculaire, CNRS, URA 24, Université Pierre et Marie Curie, 4 Place Jussieu, 75252 Paris Cedex 05, France, ELF ATOCHEM, CERDATO, 27470 Serquigny, France, and Laboratoire de Physicochimie Structurale et Macromoléculaire, CNRS, URA 278, ESPCI, 10 Rue Vauquelin, 75231 Paris Cedex 05, France

Received December 7, 1992; Revised Manuscript Received April 29, 1993

ABSTRACT: Model compounds (S_n) of stilbene-unit containing copolymers are studied and compared with compounds T_n and H_n derived from terephthalic acid and hydroquinone, respectively. They have the following structures: $\text{Ar}[\text{COOC}_6\text{H}_4\text{COO}(\text{CH}_2)_n\text{CH}_3]_2$, where $\text{Ar} = -\text{C}_6\text{H}_4\text{CH}=\text{CHC}_6\text{H}_4-$ (S_n) and $\text{Ar} = -\text{C}_6\text{H}_4-$ (T_n); $\text{Ar}[\text{OOC}_6\text{H}_4\text{COO}(\text{CH}_2)_n\text{CH}_3]_2$, where $\text{Ar} = -\text{C}_6\text{H}_4-$ (H_n). Their liquid crystalline behaviors are established by DSC, optical microscopy, and X-ray diffraction. The lower homologues in the T_n and H_n series show only a nematic phase. When the alkyl group is lengthened, both nematic and S_A phases are formed. In the higher homologues purely S_A behavior is observed, with compound H_7 exhibiting a monotropic S_C phase. All the S_n compounds studied give N and S_C phases, with compounds S_2 , S_3 , and S_6 exhibiting a S_C - S_A transition. The effects of the central unit of the mesogenic group on liquid crystal properties are illustrated by reference to compounds T_n , H_n , S_n , and N_n (containing a 2,6-disubstituted naphthalene central ring). The effects of relatively small structural changes are illustrated by reference to compounds in which the n -alkyl chains are connected to the mesogenic groups by ester (T_n , H_n), ether (T_{on} , H_{on}), and direct (T_{dn} , H_{dn}) linkages.

Introduction

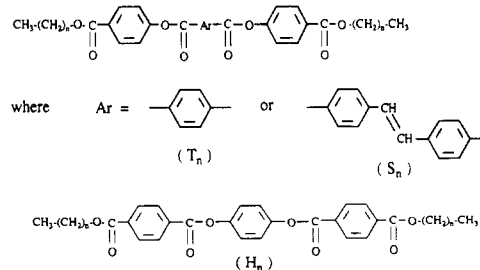
Monomer units derived from stilbenic acid (S) exhibit interesting mesogenic properties in low and high molar mass liquid crystal compounds; they are self-mesogenic and can lead to thermotropic or lyotropic polymers without the need of preforming mesogenic blocks.

Most polymers containing stilbene mesogenic groups are semiaromatic polycondensates with steadily distributed stilbene units and aliphatic segments, mainly polymethylene and polyalkylene.¹⁻¹³ The synthesis of wholly aromatic polyesters has been the subject of very few articles and patents,^{14,15} their content in stilbene units is generally low; moreover, there is little information concerning the relationships between their synthesis, their structure, and their properties.

In this series we want to discuss the interest in introducing stilbene units in copolyesters prepared from methylhydroquinone, diacids such as isophthalic, tereph-

thalic, and 4,4'-oxydibenzoic acid, and *p*-hydroxybenzoic acid.

The present paper is devoted to the study of stilbene model compounds (S_n) and to the comparison of their liquid crystalline behaviors with those of model compounds derived from terephthalic acid (T_n) and hydroquinone (H_n).



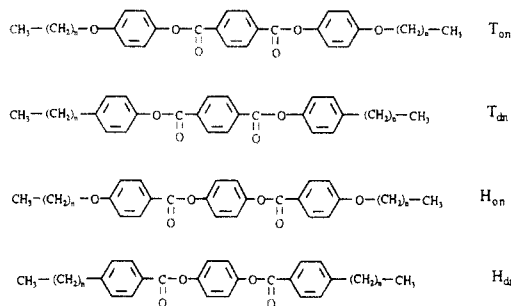
Compounds with a central terephthaloyl group were the subject of several publications;¹⁶⁻²⁴ however, some of the results led to contradictory conclusions, and it seemed important to remove these ambiguities. Both polymers H_n and T_n are of the same structure, the only difference being that in the polymers H_n the central ester linkage is placed in the chain in an alternating fashion.

[†] Laboratoire de Synthèse Macromoléculaire, CNRS.

[‡] ELF ATOCHEM, CERDATO.

[§] Laboratoire de Physicochimie Structurale et Macromoléculaire, CNRS.

The results are discussed in detail by comparing the properties of compounds S_n , T_n , and H_n to those of the following compounds described in literature: T_{on} ,¹⁹⁻²¹ T_{dn} ,²²⁻²⁴ H_{on} ,^{19a,c,23,25-28} and H_{dn} .²⁹



The synthesis and properties of the copolyesters are described in the second paper of the series.

Experimental Part

Materials. Alkyl 4-Hydroxybenzoates. Methyl ($n = 0$), ethyl ($n = 1$), and propyl ($n = 2$) 4-hydroxybenzoates are commercial compounds (Aldrich).

Higher 4-hydroxybenzoates are prepared by refluxing a mixture of 4-hydroxybenzoic acid (0.1 mol), toluene (200 mL), $CH_3-(CH_2)_nOH$ ($3 \leq n \leq 6$; 0.1 mol), and sulfuric acid (5 drops) for 5 h. Water is then eliminated through azeotropic distillation, and toluene and alkanol in excess are distilled out under reduced pressure.

T_n Compounds. A mixture of 4-hydroxybenzoate (0.1 mol), terephthaloyl chloride (0.03 mol), and freshly distilled pyridine (200 mL) is stirred at room temperature for 12 h. The reaction mixture is then poured into water (pH = 4–5). The resulting precipitate is filtered off, dissolved in chloroform, and washed with water. The organic layer is separated and evaporated, and the residual product is crystallized from ethyl acetate. Elem anal. Calcd for $C_{24}H_{18}O_8$ (T_0): C, 66.36; H, 4.18; O, 29.46. Found: C, 66.34; H, 4.20; O, 29.40. Calcd for $C_{26}H_{22}O_8$ (T_1): C, 67.53; H, 4.79; O, 27.68. Found: C, 67.53; H, 4.88; O, 27.59. Calcd for $C_{28}H_{26}O_8$ (T_2): C, 68.56; H, 5.34; O, 26.09. Found: C, 68.48; H, 5.29; O, 26.14. Calcd for $C_{30}H_{30}O_8$ (T_3): C, 69.49; H, 5.83; O, 24.68. Found: C, 69.50; H, 5.85; O, 24.56. Calcd for $C_{32}H_{34}O_8$ (T_4): C, 70.31; H, 6.27; O, 23.42. Found: C, 70.32; H, 6.23; O, 23.40. Calcd for $C_{34}H_{38}O_8$ (T_5): C, 71.06; H, 6.66; O, 22.27. Found: C, 70.87; H, 6.63; O, 22.39. Calcd for $C_{36}H_{42}O_8$ (T_6): C, 71.74; H, 7.02; O, 21.24. Found: C, 71.74; H, 7.02; O, 21.10. Calcd for $C_{38}H_{46}O_8$ (T_7): C, 72.36; H, 7.35; O, 20.29. Found: C, 72.26; H, 7.37; O, 20.35.

H_{40} . Toluyl chloride (28 g, 0.18 mol) is added dropwise to a solution of hydroquinone (6.6 g, 0.06 mol) in freshly distilled pyridine (100 mL); the temperature is maintained below 30 °C. The reaction mixture is poured into acidified water (pH = 3–4), and the resulting crude H_{40} is filtered off, washed with a 5% $NaCO_3H$ solution, and crystallized from acetic acid (yield = 68%). Elem anal. Calcd for $C_{22}H_{18}O_4$: C, 76.29; H, 5.24; O, 18.48. Found: C, 76.34; H, 5.19; O, 18.40.

H_{p1} . Oxygen (0.4 L min^{-1}) is bubbled through a mixture of H_{40} (45 g, 0.13 mol), propionic acid (1 L), $CoCl_2 \cdot 6H_2O$ (0.45 g, 1.89 mmol), $MnBr_2 \cdot 4H_2O$ (0.90 g, 3.14 mmol), and KBr (0.45 g, 3.78 mmol) which is refluxed for 10 h (135–140 °C). H_{p1} , which precipitates as the reaction progresses, is filtered off from the warm solution, washed with boiling propionic acid, and dried. H_{p1} is not further purified (yield = 90%). Elem anal. Calcd for $C_{22}H_{14}O_8$: C, 65.03; H, 3.47; O, 31.50. Found: C, 66.47; H, 3.64; O, 29.96.

H_{p2} . A mixture of H_{p1} (35.5 g, 0.08 mol), $SOCl_2$ (400 mL), and DMF (4 mL) is refluxed for 6 h. The excess $SOCl_2$ is then distilled out under vacuum, leaving a solid. Toluene (50 mL) is added and then distilled out. This procedure is repeated, and the crude product H_{p2} is then dissolved in chloroform in the presence of active charcoal. After filtration of active charcoal, chloroform is removed (yield = 72%).

H_2 and H_5 . A mixture of pyridine (5 mL) and $CH_3(CH_2)_nOH$ (20 mL) is slowly added to a chloroform (50 mL) solution of H_{p2}

(4 g). The reaction mixture is maintained at 20 °C for 12 h. The alkanol is then eliminated through steam distillation, and chloroform is distilled out. H_2 and H_5 are crystallized from ethyl acetate. Elem anal. Calcd for $C_{28}H_{26}O_8$ (H_2): C, 68.56; H, 5.34; O, 26.09. Found: C, 68.50; H, 5.35; O, 25.90. Calcd for $C_{34}H_{38}O_8$ (H_5): C, 71.06; H, 6.66; O, 22.27. Found: C, 70.86; H, 6.48; O, 22.15.

H_7 . H_{p2} (4 g) is solubilized in methylpyrrolidone (150 mL), and triethylamine (5 mL) then reacts with n -octanol (10 g, 0.77 mol). The reaction mixture is poured into water, and the precipitate is filtered off. The crude product is crystallized from ethyl acetate. Elem anal. Calcd for $C_{38}H_{46}O_8$: C, 72.36; H, 7.35; O, 20.29. Found: C, 72.40; H, 7.29; O, 20.20.

Stilbene Dichloride. Stilbene diacid³⁰ (20 g, 0.075 mol), $SOCl_2$ (119 g, 1 mol), and DMF (0.5 mL) are refluxed for 24 h. The excess $SOCl_2$ is distilled out. Toluene is added and then distilled out. This procedure is repeated, and the crude product is crystallized from toluene (700 mL) in the presence of active charcoal. The product is obtained as yellow needles (yield = 85%).

S_n Compounds. A mixture of stilbene dichloride (5 mmol), alkyl 4-hydroxybenzoate, and freshly distilled pyridine (50 mL) is stirred for 12 h at room temperature and then poured into water. The resulting precipitate is filtered off and dissolved in dichloromethane. The solution is washed with water. The organic layer is separated and evaporated. The residual product S_n is crystallized from ethyl acetate (yield = 60–65%). Elem anal. Calcd for $C_{34}H_{28}O_8$ (S_1): C, 5.00; H, 72.33; O, 22.67. Found: C, 4.96; H, 72.35; O, 22.59. Calcd for $C_{36}H_{32}O_8$ (S_2): C, 72.96; H, 5.44; O, 21.60. Found: C, 72.72; H, 5.26; O, 21.18. Calcd for $C_{38}H_{36}O_8$ (S_3): C, 73.53; H, 5.85; O, 20.62. Found: C, 73.57; H, 6.14; O, 20.28. Calcd for $C_{44}H_{48}O_8$ (S_8): C, 74.98; H, 6.86; O, 18.16. Found: C, 74.91; H, 6.83; O, 17.89.

Analytical Techniques. NMR spectra were recorded on a 250 FT Brüker spectrometer using the XHCORR impulsion sequence ($\Delta_1 = 0.5J_{C-H}$ with $J_{C-H} = 140$ or 10 Hz) in the case of 2D-NMR ^{13}C - 1H spectra.

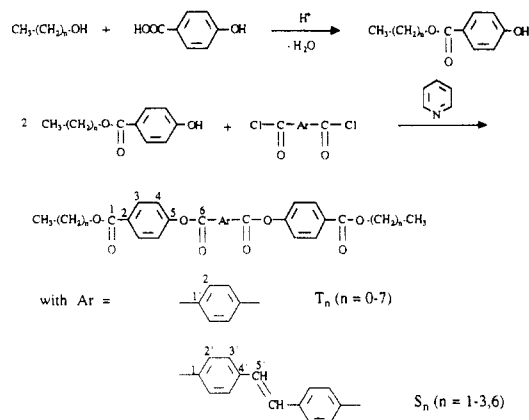
The thermal transitions were measured by means of a Du Pont 1090 thermal analyzer with a DSC 910 attachment. All samples were under 15 mg and were heated at 20 °C/min.

The transition characteristics were surveyed with a polarizing microscope (Olympus BHA-P) equipped with a Mettler FP-5 hot stage.

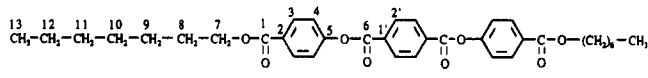
X-ray diffraction patterns were recorded on flat films using $Cu K\alpha$ radiation. A flat graphite crystal with a pinhole collimator was used as a monochromator. The samples were contained in 1-mm Lindemann glass tubes which were mounted in an electrically heated oven, the temperature of which was controlled within 0.2 °C using a platinum resistor as a sensing element.

Results and Discussion

Synthesis and Characterization of Compounds. T_n and S_n Model Compounds. They were prepared according to the following scheme:^{19a}



1H NMR spectroscopy with selective irradiation and bidimensional ^{13}C - 1H spectroscopy of these compounds were consistent with the assigned structures. The analysis

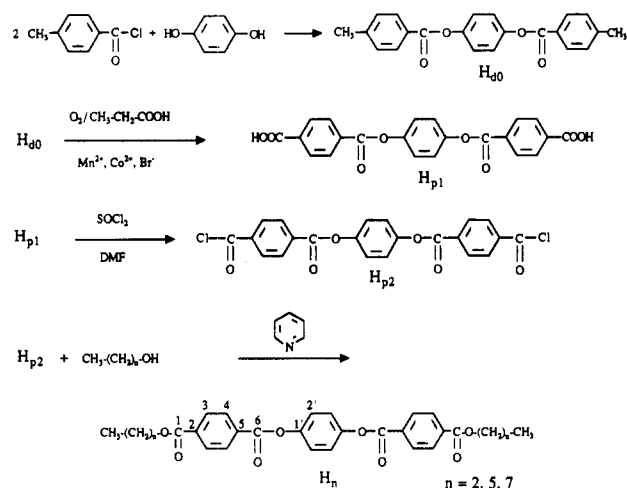
Table I. Assignments and Chemical Shifts (ppm) of T₆ ¹³C and ¹H NMR Spectra


chemical group	¹³ C		¹ H		coupling constant (Hz)
	δ (ppm)	assignment	δ (ppm)	assignment	
-CH ₃	13.80	C ¹³	0.90	H ¹³	<i>J</i> ₁₃₋₁₂ = 6.6
	22.38	C ¹²	1.32	H ¹²	
	31.54	C ¹¹	1.32	H ¹¹	
-CH ₂ -	28.74	C ¹⁰	1.37	H ¹⁰	<i>J</i> ₉₋₈ = 6.7 <i>J</i> ₈₋₇ = 6.6 ₅
	25.83	C ⁹	1.42	H ⁹	
	28.60	C ⁸	1.78 ₅	H ⁸	
	65.13	C ⁷	4.34	H ⁷	<i>J</i> ₃₋₄ = 8.8
	131.05	C ³	8.15 ₅	H ³	
	121.34	C ⁴	7.34	H ⁴	
	130.19	C ^{2'}	8.35	H ^{2'}	
	128.44	C ²			
	154.12	C ⁵			
	133.65	C ^{1'}			
	165.51	C ¹			
	163.40	C ⁶			

of the spectra permitted us to distinguish the peaks due to the 3 and 2' and to the 2 and 1' aromatic carbons, those due to the 1 and 6 carbonyl carbons, and those due to the aliphatic carbons (cf. reaction scheme).

The assignments of T₆ and S₆ spectra are given in Tables I and II.

H_n Model Compounds. They were prepared according to the following reaction scheme:^{19a,31}



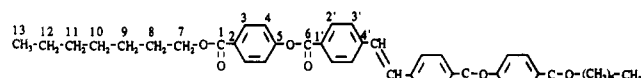
The assignments of H₇ ¹³C and ¹H NMR spectra are given in Table III.

Thermotropic Behavior. Model Compounds T_n Containing a Terephthaloyl Central Group. Table IV lists the transition temperatures of model compounds T_n.

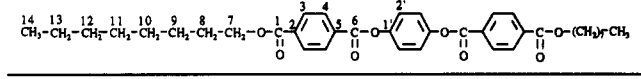
Initial classification of the phase type was based on microscopic observations of the textures exhibited by these materials. Typically, for the *n*-ethyl material, T₁, the N phase separates from the isotropic liquid on cooling in droplets; these coalesce and form a Schlieren texture (Figure 1). Cooling of this texture produces a transition to the S_A phase which is characterized by its simple focal-conic fan texture.

In the higher homologues, the S_A phase separates from the isotropic liquid, on cooling, in the form of bâtonnets (Figure 2a) which, after further cooling, coalesce and build up the focal-conic fan texture (Figure 2b).

Confirmation of the classification of the N and S_A phases was obtained by X-ray diffraction. The X-ray diffraction patterns obtained with unoriented nematic phases mainly

Table II. Assignments and Chemical Shifts (ppm) of S₆ ¹³C and ¹H NMR Spectra


chemical group	¹³ C		¹ H		coupling constant (Hz)
	δ (ppm)	assignment	δ (ppm)	assignment	
-CH ₃	13.80	C ¹³	0.90	H ¹³	<i>J</i> ₁₃₋₁₂ = 6.6
	22.46	C ¹²	1.32 ₅	H ¹²	
	31.58	C ¹¹	1.32 ₅	H ¹¹	
-CH ₂ -	28.79	C ¹⁰	1.38	H ¹⁰	<i>J</i> ₉₋₈ = 6.8 <i>J</i> ₈₋₇ = 6.6 ₅
	25.86	C ⁹	1.42	H ⁹	
	28.63	C ⁸	1.78	H ⁸	
	65.12	C ⁷	4.34	H ⁷	<i>J</i> ₃₋₄ = 8.6 <i>J</i> _{2'-3'} = 8.4
	131.02	C ³	8.14	H ³	
	121.50	C ⁴	7.32	H ⁴	
	130.63	C ^{2'}	8.22	H ^{2'}	
	126.78	C ^{3'}	7.70	H ^{3'}	
	130.34	C ^{6'}	7.33	H ^{6'}	
	128.17	C ²			
	154.46	C ⁵			
	128.52	C ^{1'}			
	141.89	C ^{4'}			
	165.70	C ¹			
	164.04	C ⁶			

Table III. Assignments and Chemical Shifts (ppm) of H₇ ¹³C and ¹H NMR Spectra


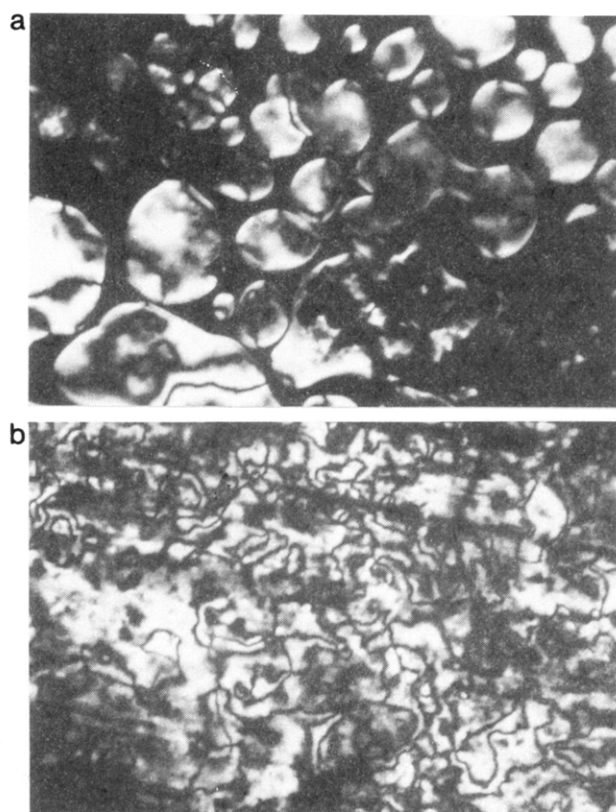
chemical group	¹³ C		¹ H		coupling constant (Hz)
	δ (ppm)	assignment	δ (ppm)	assignment	
-CH ₃	13.91	C ¹⁴	0.89	H ¹⁴	<i>J</i> ₁₄₋₁₃ = 6.6 ₅
	22.50	C ¹³	1.30	H ¹³	
	31.66	C ¹²	1.30	H ¹²	
-CH ₂ -	29.10	C ¹¹	1.33	H ¹¹	<i>J</i> ₉₋₈ = 6.8 <i>J</i> ₈₋₇ = 6.7
	29.10	C ¹⁰	1.33	H ¹⁰	
	25.92	C ⁹	1.46	H ⁹	
	28.59	C ⁸	1.81	H ⁸	<i>J</i> ₃₋₄ = 8.6
	65.60	C ⁷	4.37	H ⁷	
	129.60	C ³	8.18	H ³	
	130.00	C ⁴	8.28	H ⁴	
	122.48	C ^{2'}	7.33	H ^{2'}	
	135.01	C ²			
	132.96	C ⁵			
	148.33	C ^{1'}			
	165.58	C ¹			
	164.10	C ⁶			

show two diffuse halos (Figure 3). The outer halo is related to lateral interactions between the mesogenic cores and is found near *q* ~ 1.5 Å⁻¹ corresponding to an average molecular spacing of ~4.5–4.6 Å. The inner halo can be ascribed to intramolecular interferences. Its position corresponds to a repeat distance *d* which is slightly shorter than the molecular length *L* estimated for the most extended all-trans conformation (typically *L* - *d* = 2 Å and *L* ~ 25–30 Å).

A typical diffraction pattern for an unoriented smectic A phase is shown in Figure 4. Again the outer ring is of a diffuse nature, thus characterizing the liquidlike arrangement of molecules in the layers. The two sharp inner rings, namely a base reflection and a second-order reflection, indicate the existence of extensive layerlike correlations. For oriented smectics A, a typical diffraction pattern is shown in Figure 5. The anisotropy is clearly shown, and there are correlations of two distinct periods perpendicular and parallel to the director, which correspond to the average intermolecular spacing and to the

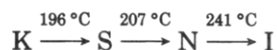
Table IV. Thermal Properties of Model Compounds T_n Containing a Terephthaloyl Central Group

model compd	transition temp (°C), Δ <i>H</i> (cal/g)
T ₀	$K \xrightarrow{248, 29.9} N \xrightarrow{302, 0.58} I$
T ₁	$K \xrightarrow{195, 22.5} S_A \xrightarrow{206, 0.48} N \xrightarrow{240, 0.32} I$
T ₂	$K \xrightarrow{130, 15.6} S_A \xrightarrow{207, 0.84} N \xrightarrow{221, 0.27} I$
T ₃	$K \xrightarrow{134, 14.6} S_A \xrightarrow{170, 1.7} I$
T ₄	$K \xrightarrow{150.5, 17.2} S_A \xrightarrow{191.6, 2.5} I$
T ₅	$K_1 \xrightarrow{94, 12.5} K_2 \xrightarrow{154, 21.3} S_A \xrightarrow{177, 3.05} I$
T ₆	$K \xrightarrow{148.5, 17.8} S_A \xrightarrow{175, 2.7} I$
T ₇	$K \xrightarrow{146, 16.7} S_A \xrightarrow{166, 2.4} I$

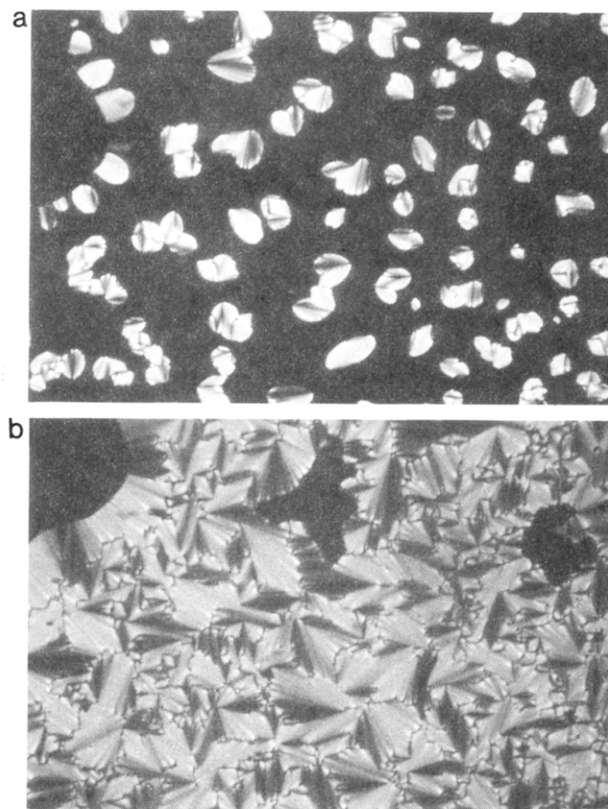
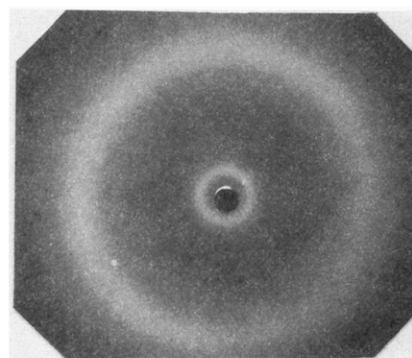
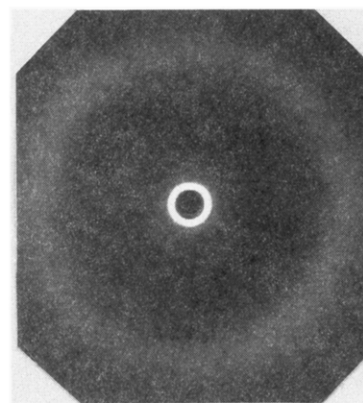
**Figure 1.** Nematic phase of T₁: (a) droplets, *T* = 239.8 °C; (b) Schlieren texture, *T* = 210 °C. Crossed polarizers (×110)

lamellar thickness. The dependence of the lamellar spacing on the alkyl chain length is given in Figure 6.

Our results are in good agreement with those reported by different authors for compounds of the same series.^{16–18} It should be noted however that only the phase transition temperatures are available in the literature. Investigations by Galli et al.¹⁶ reveal that bis[4-(ethoxycarbonyl)phenyl] terephthalate exhibits the following polymorphism:



Thermal data obtained by Bilibin et al.¹⁷ indicate that

**Figure 2.** Smectic A phase of T₅: (a) separation of the smectic A phase in the form of bâtonnets from the isotropic liquid, *T* = 176.1 °C; (b) focal-conic fan texture, *T* = 175.2 °C. Crossed polarizers (×110).**Figure 3.** Diffraction pattern for the nematic phase of T₂. *T* = 210 °C.**Figure 4.** Diffraction pattern for an unoriented sample of the S_A phase of T₇. *T* = 150 °C.

compounds T₃–T₉ form smectic mesophases while compounds T₀–T₂ could form nematic phases. Microscopic observations by Frosini et al.¹⁸ showed that bis[4-[(decyloxy)carbonyl]phenyl] terephthalate exhibits only one

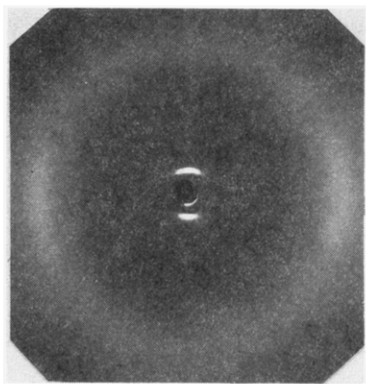


Figure 5. Diffraction pattern for an oriented sample of the S_A phase of T_2 . $T = 180\text{ }^\circ\text{C}$.

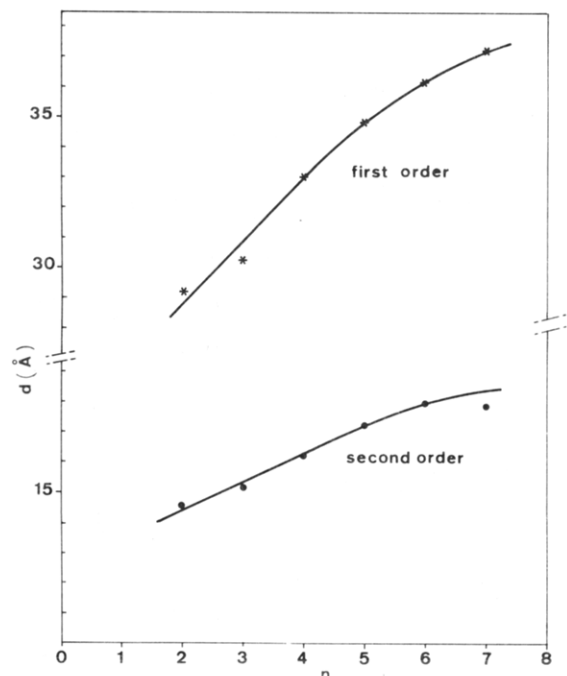


Figure 6. Dependence of the lamellar spacing, d , as a function of n -alkyl chain length.

smectic mesophase. The thermal data for compounds T_0 – T_9 are collected in Figure 7. As shown in this figure, lengthening of the alkyl end groups mainly results in the following three effects:

(1) Reduction of the clearing temperature. This reflects the decreasing thermal stability of the mesophase with decreasing polarity (or increasing n -alkane character) and molecular rigidity. Lower transition temperatures are the result of the dilution of the mesogenic groups and the increased flexibility of the molecule since the only parts of these compounds which can give rise to a large number of conformations are the alkyl end groups where each C–C bond can exist in either the trans or gauche state about the preceding C–C bond. A large number of gauche conformations present in the terminal groups distort the cylindrical shape of the mesogen and destroy the liquid crystalline order. The melting point also decreases when the alkyl group is changed from methyl to propyl. With further increase in the length of the terminal groups, the melting point increases and then levels off.

(2) An even–odd relationship for the clearing temperature in which compounds with even-numbered alkyl groups have lower transition temperatures than those with odd-numbered alkyl groups. As for many series, the melting points do not show regular trends.

(3) Change from nematic to smectic A phases. According to a common pattern of behavior in various homologous

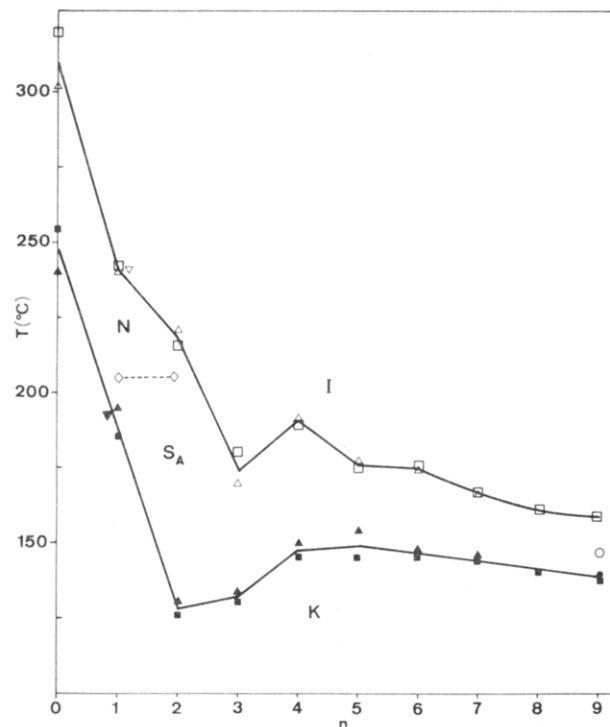


Figure 7. Thermal properties of model compounds T_n . (Δ) T_m , (\diamond) S_A – N , (Δ) T_I : this work. (∇) T_m , (∇) T_I : ref 16. (\blacksquare) T_m , (\square) T_I : ref 17. (\bullet) T_m , (\circ) T_I : ref 18.

series, the lower homologue exhibits only a nematic phase. When the alkyl group is lengthened to propyl, both nematic and smectic A phases are formed. In the higher homologues, purely smectic A behavior is observed.

The manner in which the molecules pack together in an ordered arrangement and the thermal stability of the ordered arrangement depend on the molecular structure and geometry (anisotropy, rigidity, linearity, planarity...) of the mesogenic group, the specific details of the linking group, and the equilibrium flexibility of the terminal group. Even though the change in molecular structure is quite small, the effects on liquid crystal behavior may be far reaching, and the reasons may be subtle to define. The effects of relatively small structure changes are illustrated by reference to compounds T_n , T_{on} ,^{19–21} and T_{dn} ,^{22–24} in which the alkyl chains are connected to the mesogenic groups by ester, ether, and direct linkages. The following useful observations may be made:

(1) Of the three classes of compounds under discussion, the n -alkoxy compounds, T_{on} , have the highest melting points and clearing temperatures. The latter are in the same temperature range for the systems T_{dn} and T_n (Figure 7) with the n -alkyl group attached directly to the ring and by an ester group, respectively.

(2) As the alkyl chain is lengthened, the clearing temperature decreases in an approximately even–odd, zigzag fashion. For the di- p -alkoxyphenylene terephthalates, T_{on} , the points fit two falling curves, the upper for even and the lower for odd numbers of carbon atoms in the alkyl chains. For the systems T_{dn} and T_n , the reverse situation arises. Similar trends in the clearing temperatures have been observed for a large number of homologous series.³² Such even–odd effects are induced by changes in the molecular polarizability of the molecule in its normal and perpendicular components. In the liquid crystalline state, the chain extends with some statistical preference for the regular all-trans conformation. As a result, in the compounds T_{dn} with the n -alkyl chain attached directly to the ring, the polarizability along the molecular axis is greater than that perpendicular to the

Table V. Thermal Properties of Model Compounds H_{dn} and H_n Containing a Hydroquinone Central Group

model compd	transition temp (°C), ΔH (cal/g)
H_{d0}	$K \xrightarrow{233, 31.3} N \xrightarrow{244, 1.3} I$
H_2	$T \xrightarrow{193, 18.5} K \xrightarrow{211, 0.28} N \xrightarrow{211, 0.28} I$ $T \xrightarrow{126.5} K \xleftarrow{139.5} S_A \xleftarrow{211} N \xleftarrow{211} I$
H_5	$K \xrightarrow{129^a} S_A \xrightarrow{135^a} N \xrightarrow{150, 0.24} I$
H_7	$T \xrightarrow{60, 7.6} K_1 \xrightarrow{126^b} K_2 \xrightarrow{136^b} S_A \xrightarrow{140.5^b} N \xrightarrow{140.5^b} I$ $T \xrightarrow{124.7} K \xleftarrow{130.8} S_C \xleftarrow{133.5} S_A \xleftarrow{139.5} N \xleftarrow{139.5} I$

^a Overlapping peaks; total enthalpy change $\Delta H = 9.25$ cal/g.

^b Overlapping peaks; total enthalpy change $\Delta H = 17.9$ cal/g.

axis for alkyl chains with an odd number of carbon atoms but is about equal for alkyl chains with an even number of carbon atoms. Stronger attractions exist between the mesogens with odd-numbered alkyl chains, and, consequently, these compounds have higher clearing temperatures. For esters, the COO group is equivalent to the two first CH_2 groups next to the ring, which explains why compounds T_n also show this trend. For ethers, however, the O atom replaces the first CH_2 group next to the ring, and, as a consequence, the even members are on the upper curve.

(3) As observed for compounds T_n with ester links, the di-*p*-alkoxyphenylene terephthalates, T_{on} , exhibit smectic mesophases for higher alkyl chain lengths. It should be noted, however, that the tendency for purely nematic behavior is observed when the alkyl group is changed from methyl to ethyl and from butyl to pentyl in compounds T_n and T_{on} , respectively. These results suggest that ring-COO bonds enhance smectic thermal stabilities. It is obvious that dipole moments acting across the long molecular axis may strongly favor smectic behavior, and for this reason compounds with terminal ring-COOR functions are inclined to be smectogenic. When a direct link between the alkyl group and the mesogenic unit is used, the resulting derivatives form only nematic mesophases to the best of our judgment from the scarce data available in the literature.

Model Compounds H_n and H_{dn} Containing a Hydroquinone Central Group. The transition temperatures for these compounds are listed in Table V. Microscopic observations indicate the existence of N, S_A , and S_C phases depending on the chemical structure. Upon cooling from the isotropic state, the nematic phase begins to separate in the form of droplets which, after further cooling, join together and result in a Schlieren texture (Figure 8). Thin layers exhibit other nematic characteristics such as scintillation effects and a marked tendency to be homeotropic. On cooling the nematic phase of H_2 , H_5 , and H_7 , a transition to the S_A phase takes place, and a transient striated texture with typical transition bars forms (Figure 9). This texture changes on standing for some times into the stable homeotropic and focal conic fan textures (Figure 10). There is some indication that H_7 forms a S_C phase at lower temperature. Indeed, on cooling the S_A phase a transition takes place with the fans becoming broken and mottled in appearance. The homeotropic areas become birefringent and exhibit a Schlieren texture (Figure 11).



Figure 8. Schlieren texture of the nematic phase of H_7 . $T = 136.7$ °C. Crossed polarizers ($\times 110$).

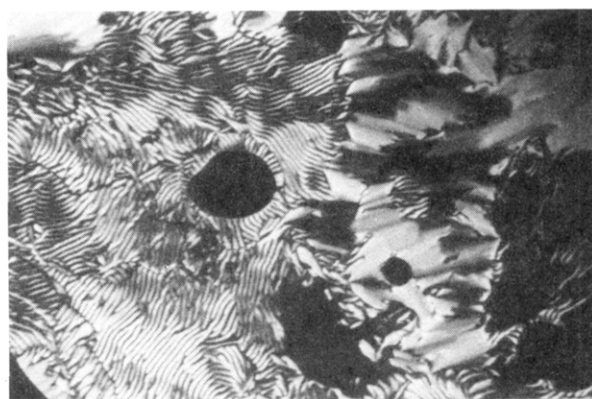


Figure 9. Transition nematic/ S_A for H_7 . $T = 133.5$ °C. Crossed polarizers ($\times 110$).

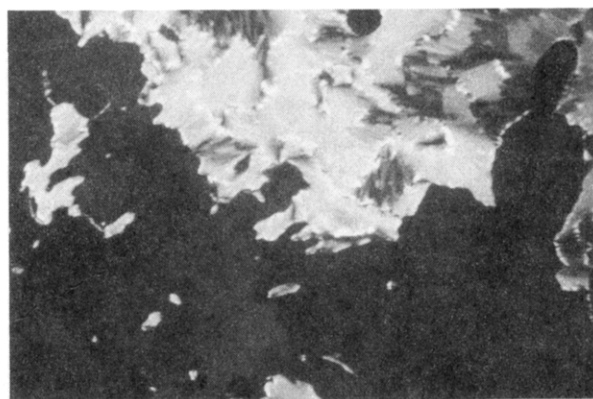


Figure 10. Focal-conic fan and homeotropic textures of the smectic A phase of H_7 . $T = 132.5$ °C. Crossed polarizers ($\times 110$).

The assignment of stable enantiotropic N and S_A phases was confirmed by X-ray diffraction. The X-ray patterns obtained for compounds H_{dn} and H_n are quite similar to those previously described for compounds T_n . In particular, in the S_A state, the d spacings of the layers are found to be almost identical for each pair of analogs. For example, the layer thickness is 33.82 Å for H_5 and 34.84 Å for T_5 .

The data from Table V are presented graphically in Figure 12. In relation to polymorphism, it is also of interest to recall the behavior of the compounds H_{dn} (Table V)²⁹ and H_{on} ,^{19a,c,23,25-28} with the n -alkyl group attached directly to the ring or by an ether group. The results parallel the trends in liquid crystal thermal stability with increasing length of the n -alkyl chain already discussed for the model compounds containing a terephthaloyl central group, particularly the regular changes in clearing points between odd and even carbon number homologues. Again for n -alkyl ethers, H_{on} , the clearing points fit two falling curves,

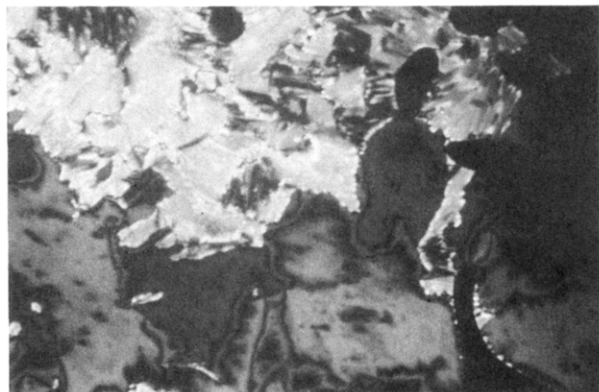


Figure 11. Broken focal-conic fan and Schlieren textures of the smectic C phase of H_7 . $T = 130.6^\circ\text{C}$. Crossed polarizers ($\times 110$).

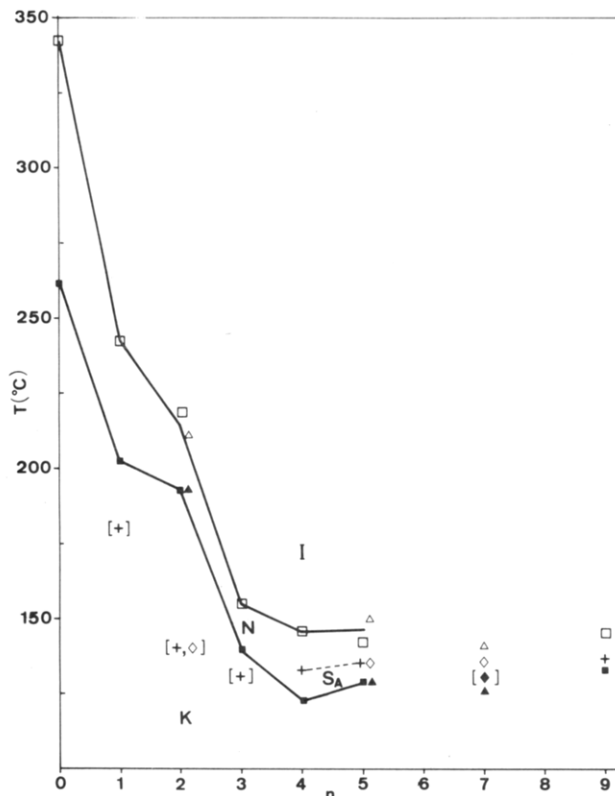


Figure 12. Thermal properties of compounds H_n . [] Monotropic transition. (■) T_m , (+) S-N, (□) T_1 ; refs 19a and 33. (▲) T_m , (◆) S_C - S_A , (◇) S_A -N, (Δ) T_1 ; this work.

the upper for even and the lower for odd numbers of carbon atoms in the n -alkyl chain. The reverse situation arises for the systems H_{dn} and H_n with the n -alkyl group attached directly to the ring or by an ester group, respectively. The n -alkyl ethers, H_{on} , give rise to liquid crystals which are more thermally stable than those formed by compounds H_{dn} and H_n . However, direct attachment of an alkyl group to the aromatic ring strongly represses smectic properties relative to those for ring-O bonds and to a greater extent, ring-COO bonds. For example, when the alkyl group = C_8 ($n = 7$), the system with a direct link is purely nematic; the corresponding system with a ring-O bond gives $T_{K-S_C} = 121^\circ\text{C}$, $T_{S_C-N} = 125^\circ\text{C}$, $T_{N-I} = 193.5^\circ\text{C}$; the ester exhibits smectic A and N phases ($T_{K-S_A} = 126^\circ\text{C}$, $T_{S_A-N} = 136^\circ\text{C}$, $T_{N-I} = 140.5^\circ\text{C}$) and shows in addition a monotropic S_C phase (Table V).

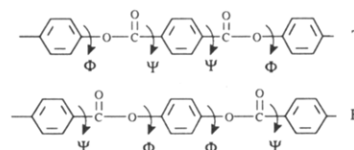
In relation to the results for the model compounds with a terephthaloyl central group and for the systems with a hydroquinone central residue, the following useful observations may be made:

(1) The clearing points for the p -phenylene di- p -alkoxybenzoates, H_{on} , are slightly higher than those for the corresponding p -alkoxyphenyl terephthalates, T_{on} , implying that for each pair of analogs, the isomer H_o forms the more stable mesophase.

The isomers H_{on} have lower melting points than those of the series T_{on} . As a result, temperature ranges of mesophase stability, ΔT , are increased in the former. As pointed out by Dewar and Goldberg,^{19a} in the p -phenylene di- p -alkoxybenzoates, H_{on} , there is mutual conjugation between the alkoxy and carboxy groups; this should increase the polarity of the carbonyl oxygen and so help to stabilize the mesophase. In the corresponding p -alkoxyphenyl terephthalates, T_{on} , such mutual conjugation is lacking; this could explain why, for each pair of analogs, the isomer H_o forms the more stable mesophase.

(2) Similar trends are observed for the series H_{dn} and T_{dn} , but the situation is the opposite for the systems H_n and T_n . Indeed, as can be seen from Figures 7 and 12, the model compounds containing a terephthaloyl central residue, T_n , provide liquid crystals which are more thermally stable than those of the analogs, H_n . A problem is that the polymorphism is not the same for these two series. In the T_n series, the C_1 member ($n = 0$) is purely nematic but the C_2 ($n = 1$) and C_3 ($n = 2$) members exhibit both nematic and smectic A mesophases, with the higher homologues giving only smectic A mesophases. On the other hand, in the H_n series, no smectic properties occur up to and including the C_4 ($n = 3$) member. The higher homologues exhibit both nematic and smectic mesophases.

At least four features of the molecules have been thought to contribute to mesophase stability, i.e., rigidity, linearity, polarizability, and enhancement of polarity by conjugation. In this regard it is important to note that the geometries of the mesogenic groups T and H are not the same.



X-ray crystallographic data reported for benzoate and terephthalate esters³⁴⁻³⁷ indicate that the internal rotation angles Ψ_i which define the orientation of an aromatic ring with respect to the adjacent carboxyl groups are confined to values near 0° and 180° . The observed deviations are usually less than 10° . On the basis of experimental evidence³⁸⁻⁴⁰ and from the conclusions drawn from conformational energy calculations,⁴¹⁻⁴⁴ the torsional angles involving phenylene groups in type H compounds can be assumed to be $\Phi_i = \pm 60-65^\circ$ and $\Psi_i = 0$ or 180° . In type T compounds, the central terephthalate unit can be assumed to be planar, and the torsional angle Φ_i , equal to $\pm 60-65^\circ$. At the melting point, the conformation of the central terephthalate unit will remain unchanged because of relatively restricted rotation about the ring-COO bond. If the crystal preceding the mesophase adopts a layered lattice, the lateral intermolecular attractions will remain able to keep the lateral arrangement in the liquid crystalline state, hence stabilizing smectic mesophases.

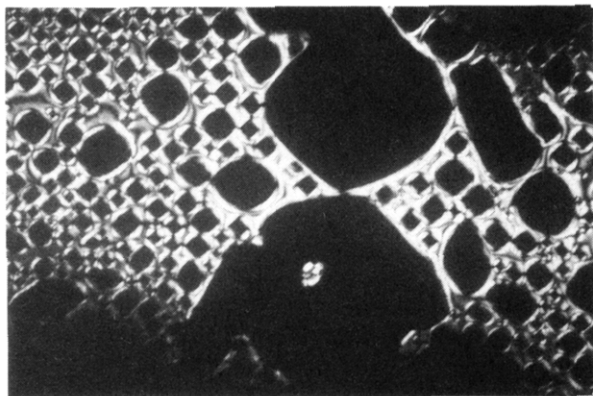
Model Compounds S_n Containing a Stilbene Central Group. The transition temperatures for the model compounds S_n are listed in Table VI.

Initial classification of the phase type was based on microscopic observations of the textures exhibited by these materials. All the S_n compounds studied give N and S_C phases, with the compounds S_2 , S_3 , and S_6 exhibiting a S_C - S_A transition. The nematic phases formed from the isotropic liquid possess two textural forms, namely, the

Table VI. Thermal Properties of Model Compounds S_n Containing Stilbene Groups

model compd	transition temp ($^{\circ}\text{C}$), ΔH (cal/g) ^a			
S_1	$\text{K} \xrightarrow{191.6, 18.1} \text{S}_\text{C} \xrightarrow{223-225} \text{N} \xrightarrow{320-340} \text{I}$			
S_2	$\text{K}_1 \xrightarrow{112, 3.0} \text{K}_2 \xrightarrow{136.5, 14.2} \text{S}_\text{C} \xrightarrow{250-260} \text{S}_\text{A} \xrightarrow{270-280} \text{N} \xrightarrow{303-320} \text{I}$			
S_3	$\text{K} \xrightarrow{135.3, 13.5} \text{S}_\text{C} \xrightarrow{240-245} \text{S}_\text{A} \xrightarrow{265-270} \text{N} \xrightarrow{282-290} \text{I}$			
S_6	$\text{K}_1 \xrightarrow{114, 0.75} \text{K}_2 \xrightarrow{129, 19.7} \text{S}_\text{C} \xrightarrow{220-230} \text{S}_\text{A} \xrightarrow{<285} \text{N} \xrightarrow{\quad} \text{I}$			

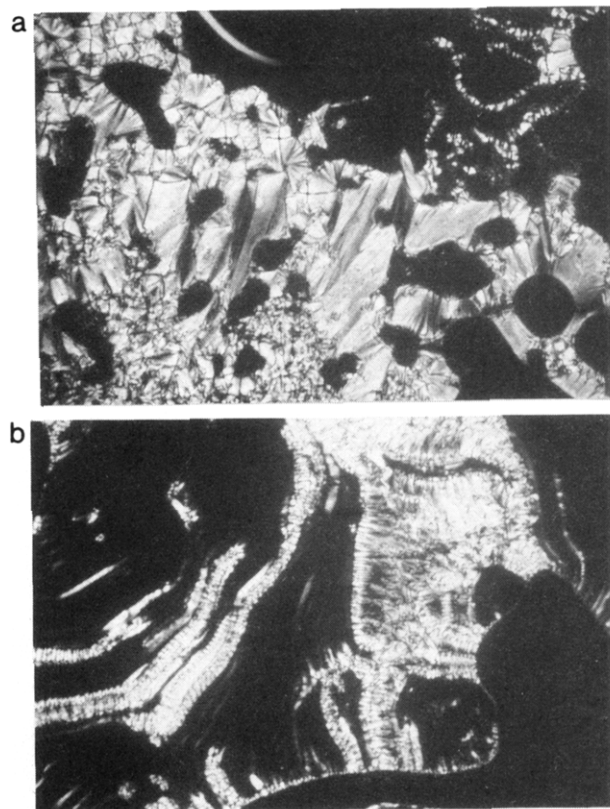
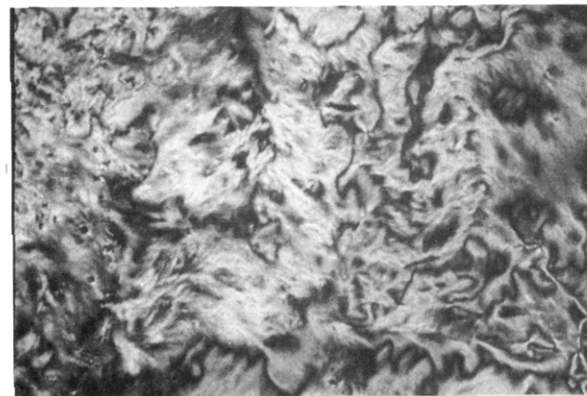
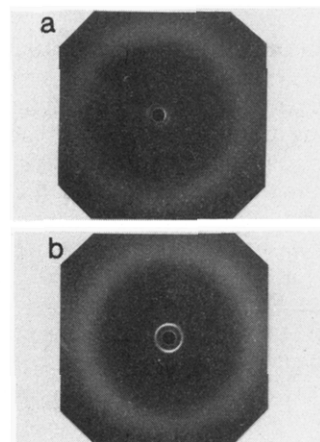
^a The enthalpies associated with the S_C - S_A , S_A - N , and N - I transitions are so small that these transitions are undetected by DSC. Accordingly, the transition temperatures are those corresponding to microscopic observations.

**Figure 13.** Nematic-isotropic liquid transition of S_6 . Crossed polarizers ($\times 110$).

Schlieren and the homeotropic texture. At the isotropic liquid-mesophase transition droplets are observed, but they are transient and give way rapidly to the formation of the Schlieren texture. The nematic sparkling phenomenon is also clearly observed. The smectic A phases adopt one of the two textures, the focal-conic fan-shaped or homeotropic texture. Occasionally it is possible to observe oily streaks which appear as bright bands or ribbons starting from air bubbles in the dark homeotropic regions. At the S_A - S_C transition a Schlieren texture is obtained from the clear focal-conic texture of the preceding A phase. It should be noted that the birefringence colors of the Schlieren texture change with temperature, which is due to tilt angle changes. Typical textures are shown in Figures 13-15.

Confirmation of the classification of the N , S_A , and S_C phases was obtained by X-ray diffraction. Typically, the X-ray patterns obtained with powder samples of these materials in the nematic state consist of the broad, diffuse halo related to the lateral spacing between mesogenic groups. It corresponds to an average intermolecular spacing of approximately 4.7-4.8 Å. The X-ray diffraction patterns obtained for S_1 , which has a S_C - N transition, have an additional diffuse ring at small angles. It corresponds to a distance of about 31 Å at 230 $^{\circ}\text{C}$ which is less than the molecular length calculated for the molecule in the fully extended, all-trans conformation ($L \approx 33$ Å). This indicates the existence of cybotactic groups having a tilt angle of about 20 $^{\circ}$.

The X-ray patterns obtained in the S_A state have a diffuse outer ring reflecting the absence of order within the layer planes and a sharp inner ring which can be attributed to the regular packing of smectic layers (Figure

**Figure 14.** Focal-conic fan (a) and homeotropic (b) textures of the smectic A phase of S_6 . Crossed polarizers ($\times 110$).**Figure 15.** Schlieren texture of the smectic C phase of S_6 . Crossed polarizers ($\times 110$).**Figure 16.** X-ray diffraction patterns of the S_A (a) and S_C (b) phases of S_3 .

16a). As observed for numerous low molar mass smectic A, the smectic layers are shorter than the corresponding extended molecular lengths (L) (e.g., $d/L \approx 0.97/1$), which

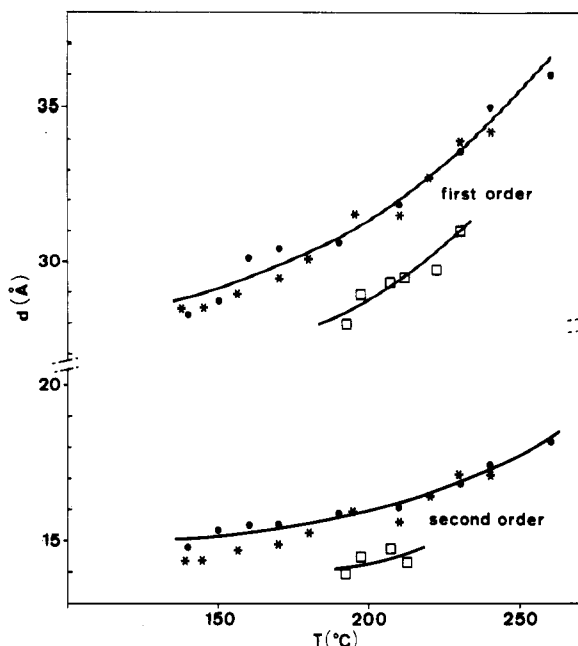
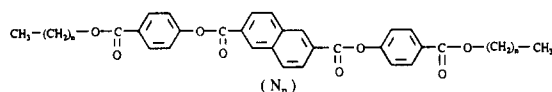


Figure 17. Change in lamellar spacing, d with temperature. (\square) S_1 ($L \approx 33$ Å); ($*$) S_2 ($L \approx 35$ Å); (\bullet) S_3 ($L \approx 37$ Å).

suggests that the molecules are randomly tilted within the individual layers, with the tilt angle varying from 10 to 15°.

In the S_C phases, the X-ray diffraction patterns are essentially the same as those for the S_A phases except that two inner rings are observed, namely, a base reflection and a second-order reflection (Figure 16b). They correspond to d -spacings much shorter than the extended molecular lengths L indicating that the molecular long axes are tilted with respect to the layer planes. It should be noted that the tilt angle θ in the C phase of the S_2 , S_3 , and S_6 compounds decreases with increasing temperature in a uniform way, changing gradually from 35–40° at low temperatures to about 10–15° at the S_C – S_A transition. Typical lamellar spacing, d , or tilt angle, θ , vs temperature plots are given in Figure 17. The S_C phase of S_1 does not have a wide enough temperature range for the change in the tilt angle to be easily detected by measurements of lamellar spacings. In addition, as previously mentioned, S_1 exhibits a S_C –N transition. For this compound the tilt angle decreases from about 32° to 20°, the tilt angle determined for cybotactic groups in the N phase.

Information about the effects of the central unit of the mesogenic group on liquid crystal properties are illustrated by reference to compounds T_n , S_n , and N_n containing a 1,4-disubstituted ring, a stilbene group, and a 2,6-disubstituted naphthalene ring,¹⁷ respectively.



In accordance with the general requirement of an elongated and fairly rigid molecular structure, derivatives of stilbene, S_n , provide liquid crystals which are much more thermally stable than those of the benzene analogues; cf. the clearing temperatures for compounds S_n (Table VI) and T_n (Table IV and Figure 7). This points out the importance of the rigid nature of the geometry of stilbene in stabilizing liquid crystals. Indeed, the linking unit $-\text{CH}=\text{CH}-$ contains a double bond about which freedom of rotation is restricted, so preserving the rigidity and

elongation of the molecules. Besides, systems involving this linking unit are planar. Replacement of the 1,4-disubstituted benzene ring by a 2,6-disubstituted naphthalene ring giving N_n gives clearing temperatures intermediate between those for compounds T_n and S_n , consistent with the molecule having been elongated but broadened.

References and Notes

- (1) Toland, W. G. U.S. Patent 2,657,195, 1953.
- (2) Parham, F. M. U.S. Patent 3,361,716, 1968.
- (3) Jackson, W. J.; Morris, J. C. *J. Appl. Polym. Sci., Appl. Polym. Symp.* 1985, 41, 307.
- (4) Jackson, W. J.; Morris, J. C. *J. Polym. Sci., Polym. Chem. Ed.* 1987, 25, 575.
- (5) Roviello, A.; Santagata, S.; Sirigu, A. *Makromol. Chem., Rapid Commun.* 1984, 5, 141.
- (6) Carfagna, C.; Roviello, A.; Santagata, S.; Sirigu, A. *Makromol. Chem.* 1986, 187, 2123.
- (7) Morris, J. C.; Jackson, W. J. U.S. Patent 4,459,402, 1984.
- (8) Morris, J. C.; Jackson, W. J. U.S. Patent 4,420,607, 1983.
- (9) Jackson, W. J.; Morris, J. C. *J. Polym. Sci., Polym. Chem. Ed.* 1988, 26, 835.
- (10) Morris, J. C.; Jackson, W. J. U.S. Patent 4,414,382, 1983.
- (11) Morris, J. C.; Jackson, W. J. U.S. Patent 4,551,520, 1985.
- (12) Morris, J. C.; Jackson, W. J. U.S. Patent 4,728,719, 1988.
- (13) Morris, J. C.; Jackson, W. J. U.S. Patent 4,728,717, 1988.
- (14) Schaeffgen, J. R. U.S. Patent 4,118,372, 1978.
- (15) Calundann, G. W.; Rasoul, H. A. A.; Hall, H. K. U.S. Patent 4,654,412, 1987.
- (16) Galli, G.; Chiellini, E.; Ober, C. K.; Lenz, R. W. *Makromol. Chem.* 1982, 183, 2693.
- (17) Bilibin, A. Yu.; Tenkovtsev, A. V.; Piraner, O. N.; Pashkovsky, E. E.; Skorokhodov, S. S. *Makromol. Chem.* 1985, 186, 1575.
- (18) Frosini, V.; de Petris, S.; Chiellini, E.; Galli, G.; Lenz, R. W. *Mol. Cryst. Liq. Cryst.* 1983, 98, 223.
- (19) (a) Dewar, M. J. S.; Goldberg, R. S. *J. Org. Chem.* 1970, 35 (8), 2711. (b) Dewar, M. J. S.; Riddle, R. M. *J. Am. Chem. Soc.* 1975, 97 (23), 6658. (c) Dewar, M. J. S.; Griffin, A. C. *J. Am. Chem. Soc.* 1975, 97 (23), 6662.
- (20) Kelker, H.; Scheurle, B. *J. Phys. (Paris)* 1969, 30, C4, 104.
- (21) Verbit, L.; Tuggey, R. L. *Mol. Cryst. Liq. Cryst.* 1972, 17, 49.
- (22) Fradet, A.; Heitz, W. *Makromol. Chem.* 1987, 188, 1233.
- (23) Deutscher, H. J.; Vorbrodt, H. M.; Zschke, H. *Z. Chem.* 1981, 21, 9.
- (24) Judas, D.; Jungblut, C.; Cuzin, D.; Friedrich, C.; Noël, C. unpublished data.
- (25) Arora, S. L.; Ferguson, J. L.; Taylor, T. R. *J. Org. Chem.* 1970, 35, 4055.
- (26) Schroeder, J. P. *Mol. Cryst. Liq. Cryst.* 1980, 61, 229.
- (27) Haut, S. A.; Schroeder, D. C.; Schroeder, J. P. *J. Org. Chem.* 1972, 37, 1425.
- (28) Dewar, M. J. S.; Goldberg, R. S. *J. Am. Chem. Soc.* 1970, 92 (6), 1582.
- (29) Demus, D.; Demus, H.; Zschke, H. In *Flüssige Kristalle in Tabellen*; VEB Deutscher Verlag für Grundstoffindustrie: Leipzig, 1974; p 81.
- (30) Toland, W. G.; Wilkes, J. B.; Brutschy, F. J. *J. Am. Chem. Soc.* 1953, 75, 2263.
- (31) McIntyre, J. E. *Br. Patent* 978,600, 1962.
- (32) Gray, G. W. In *Liquid Crystals and Plastic Crystals*; Gray, G. W., Winsor, P. A., Eds.; Ellis Horwood: Chichester, U.K., 1974; Chapter 4, p 103. *Polymer Liquid Crystals*; Ciferri, A., Krigbaum, W. R., Meyer, R. B., Eds.; Academic Press: New York, 1982; Chapter 1, p 1.
- (33) Dewar, M. J. S.; Schroeder, J. P. *J. Org. Chem.* 1965, 30, 2296.
- (34) Briese, F.; Perez, S. *Acta Crystallogr., B* 1976, 32, 470, 1518, 2110; 1977, 33, 1673, 3259; *Can. J. Chem.* 1975, 53, 3551.
- (35) Kashino, S.; Haisa, M. *Acta Crystallogr., B* 1975, 31, 1819.
- (36) Krigbaum, W. R.; Barber, P. G. *Acta Crystallogr., B* 1971, 27, 1884.
- (37) Bailey, M. *Acta Crystallogr.* 1949, 2, 120.
- (38) Saiz, E.; Hummel, J. P.; Flory, P. J.; Plavsic, M. *J. Phys. Chem.* 1981, 85, 3211.
- (39) Adams, J. M.; Morsi, S. E. *Acta Crystallogr., B* 1976, 32, 1345.
- (40) Sedlacek, P.; Stokr, J.; Schneider, B. *Collect. Czech. Chem. Commun.* 1981, 46, 1646.
- (41) Hummel, J. P.; Flory, P. J. *Macromolecules* 1980, 13, 479.
- (42) Bicerano, J.; Clark, H. A. *Macromolecules* 1988, 21, 585, 597.
- (43) Meurisse, P.; Lauprêtre, F.; Noël, C. *Mol. Cryst. Liq. Cryst.* 1984, 110, 41.
- (44) Tonelli, A. F. *J. Polym. Sci., Part B* 1973, 11, 441.